Research Academy for Young Scientists

Computationally Modeling Gamma-ray Burst Afterglow Synchrotron Emission

Marcell Ziegler
marcell.ziegler.22@gmail.com

under the direction of
Dr. Nikhil Sarin
Stockholm University
Nordita

July 12, 2023

*

Abstract

This study summarises two models of gamma-ray burst (GRB) afterglow modelling: a historic spherical model by Sari, Piran, and Narayan [1] and an early jet model by Sari, Piran, and Halpern [2]. Despite that research has proven the spherical model incorrect, it is included to give a holistic representation of the field. The spectral flux derived from the models is plotted with example parameters to illustrate how GRB light curves behave. Relativistic beaming and its effect on light from GRB jets in also discussed. Furthermore, a brief history of GRB physics and their significance in an astrophysical context is given as well as a discussion on future research opportunities.

Acknowledgements

There have been a lot of amazing people who have made this project possible. Primarily, I want to thank my mentor and supervisor, Dr. Nikhil Sarin, who has guided me through the perils of relativistic physics with a steady hand. This project would not have been possible without him or the work of the Rays team. Max Eriksson, Linnea Jonröd, Julia Mårtensson and Viktor Sundström have all done a wonderful job of making sure that this reasearch program went smoothly. I also want to extend my thanks to every Rays alumnus, every xRay, that has contributed to this study with their brutal yet constructive criticism. Furthermore, I would like to thank the partners of Rays, specifically the Magnus Bergvall Foundation and the Beijer Foundation for their support in making this happen. Finally, I want to thank all of my peers at Rays, they have made this the best summer of my life and I will never forget them.

Contents

Glossary

afterglow Delayed broadband emission from a GRB after the prompt emission.

light curve A plot of the total spectral flux of an object over time.

prompt emission The initial burst of gamma-rays from a GRB.

spectral flux Energy per unit time per unit area for a certain frequency.

spectrum In this context, it has two meanings: (i) the distribution of spectral flux for all frequencies at a given time and (ii) the range of radiation frequencies possible, as in "EM spectrum".

stellar mergers The collision and merging of two stars or a star and another massive object.

1 Introduction

A gamma-ray burst (GRB) is a transient, explosive, astronomical event that follows some compact stellar mergers and collapses of massive stars. They are observed as bright gamma-ray flashes followed by fainter broadband radiation referred to as afterglow. GRBs are some of the brightest, most energetic explosions in the universe since the big bang [3, Ch. 1]. The duration of the flash itself, the prompt emission, is categorised into two distinct categories: short and long. The flash duration is quantified by the time T_{90} which is the time it takes for 90 % of the energy to be released. If T_{90} is $\sim$2 s or less, the burst is short, otherwise it is long [4]. This flash is followed by the fainter afterglow emission which can be viewed longer, sometimes for hundreds of days [5].

The duration of GRB prompt emission is related to the source of the explosion [3, Ch. 2]. It is believed that long GRBs are created during massive star collapse. This discovery

was made by finding supernova spectra embedded in GRB spectra and by detecting non-GRB, supernova-specific emission from the same location as a gamma-ray burst [e.g. 6], [3, Ch. 2].

In the case of short GRBs, research posits that they are related to mergers of compact stellar objects [3, Ch. 2]. These mergers are referred to as kilonovae. The kilonova-GRB relation is studied in a similar way to the supernova-GRB relation: by comparing the measured spectrum and gravitational wave observations with what is expected in theory [e.g. 7].

1.1 History

The first GRB was discovered in 1967 by the Vela satellites and the results were published by Klebesadel, Strong, and Olson [8]. Thirty years later the first afterglow was observed by Costa, Frontera, Heise, *et al.* [5]. Despite knowing about afterglows for a much shorter time, they are better understood than prompt emission.

In the case of afterglows, it was initially thought that the ejected material from the explosion—the ejecta—expanded in a spherical manner from the epicenter of the explosion. It would then interact relativistically with the surrounding interstellar medium (ISM) and create synchrotron and inverse Compton radiation [1], [9]. This study is only concerned with the former, the emission mechanism of which is described in Section 2. Currently, it is known that this spherical model of ejecta expansion is incorrect [9]. Instead, it has been found that GRB ejecta expand in the shape of two polar jets. One of the first jet models was presented by Sari, Piran, and Halpern [2].

To this day, the understanding of how the prompt emission occurs is limited. In a 2012 review, Gehrels and Mészáros [9] discuss a theory that the debris from the explosion forms a rotating disc which accretes material onto the explosion remnant—an accretion disc. This accretion powers two jets of ejected material originating from the poles of the remnant. During the time between the jets forming and them reaching the surrounding interstellar material, prompt emission of gamma-rays occurs. This is due to certain, mostly unknown, physical processes in the jets. When the jets reach the ISM, they shock it

and create afterglow radiation. Since there is currently no direct method to observe the processes involved in creating prompt emission, it is hard to prove this theory.

1.2 Physics of the Afterglow

The bulk of afterglow emission is generated by relativistic interactions near the boundary between the ejecta and the ISM. In the case of the spherical expansion, the ejecta would propagate like in Fig. 1a. In the case of a jet model, the propagation would be as seen in Fig. 1b.

This study focuses on the synchrotron radiation in the boundary layer between the ejecta and ISM. Synchrotron radiation is a type of radiation emitted when electrons are gyrating at relativistic velocities through a strong magnetic field, as illustrated in Fig. 3. This is achieved in GRB afterglows for two reasons: (i) That the remnant of the explosion is highly charged and rotating thus generating a magnetic field and (ii) that the ejecta is moving near the speed of light away from the core of the explosion [9].

Synchrotron emission has a very broad spectrum [10]. This means that it can be viewed from short radio waves to weak gamma-rays. The approximate spectrum is shown in Fig. 2. This broadband emission makes the GRB afterglows visible to many different instruments.

1.3 Relativistic Motion

The Lorentz factor, γ is a quantity that describes the extent of special relativity's effect on an object moving at a certain velocity v. It is defined as

$$\gamma = \frac{1}{\sqrt{1 - \frac{v^2}{c^2}}}$$

where c is the speed of light in vacuum. As an example of its use, consider a clock moving relativistically at $v = 0.999c$. This corresponds to a Lorentz factor $\gamma \approx 22.4$. Now consider the time Δt_{clock} between two ticks of the clock measured in its own rest frame. This time corresponds to a time $\Delta t_{\text{observer}}$ from the observer relative to which the clock is moving

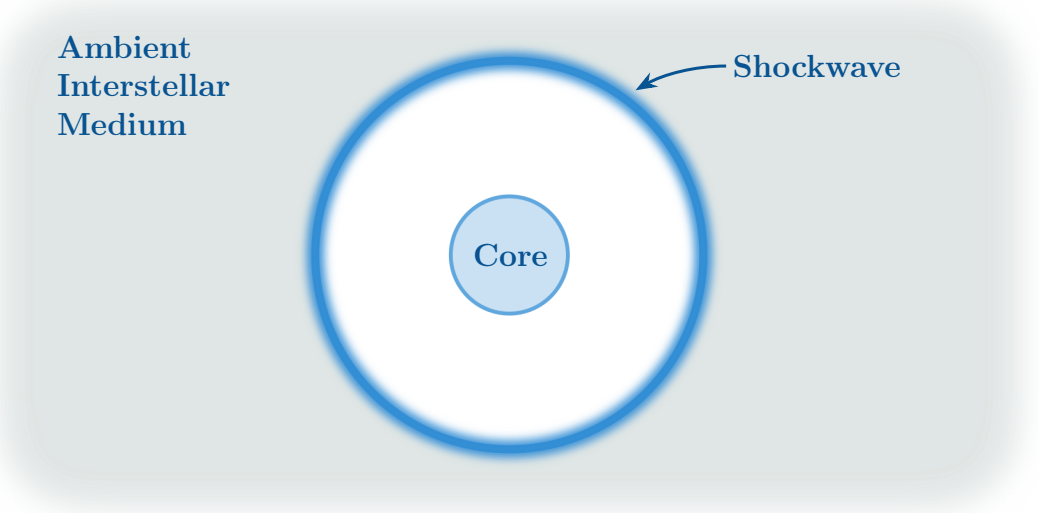

(a) Cross section of a spherical GRB explosion. Ejecta is propagating outward in a uniform sphere. The shockwave interacts with the ambient material and emits afterglow radiation.

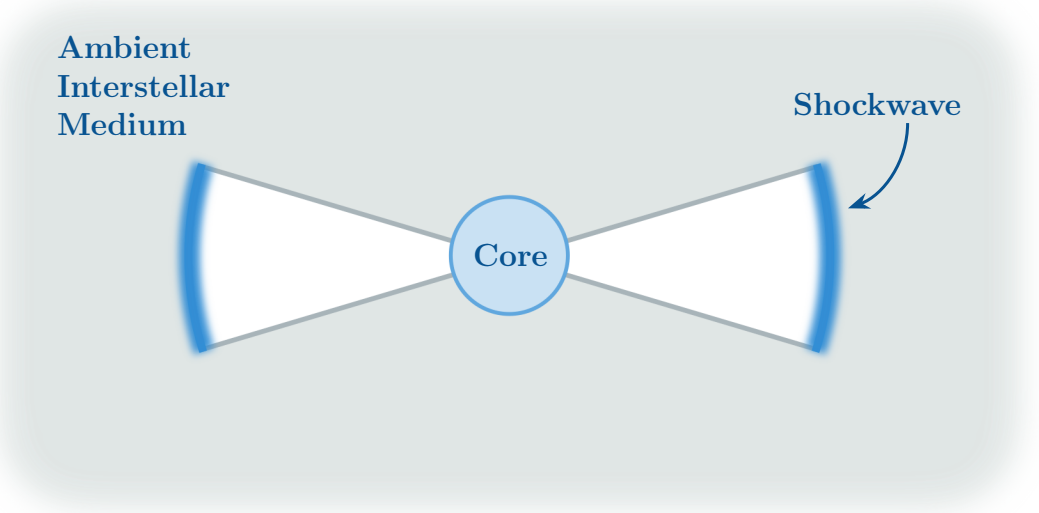

(b) Cross section of a jet-modelled GRB explosion. The ejecta expands in two conical jets from the poles of the core. The shockwaves interacts with the ambient material and emits afterglow radiation.

Figure 1: Illustration of the two models of GRB ejecta expansion.

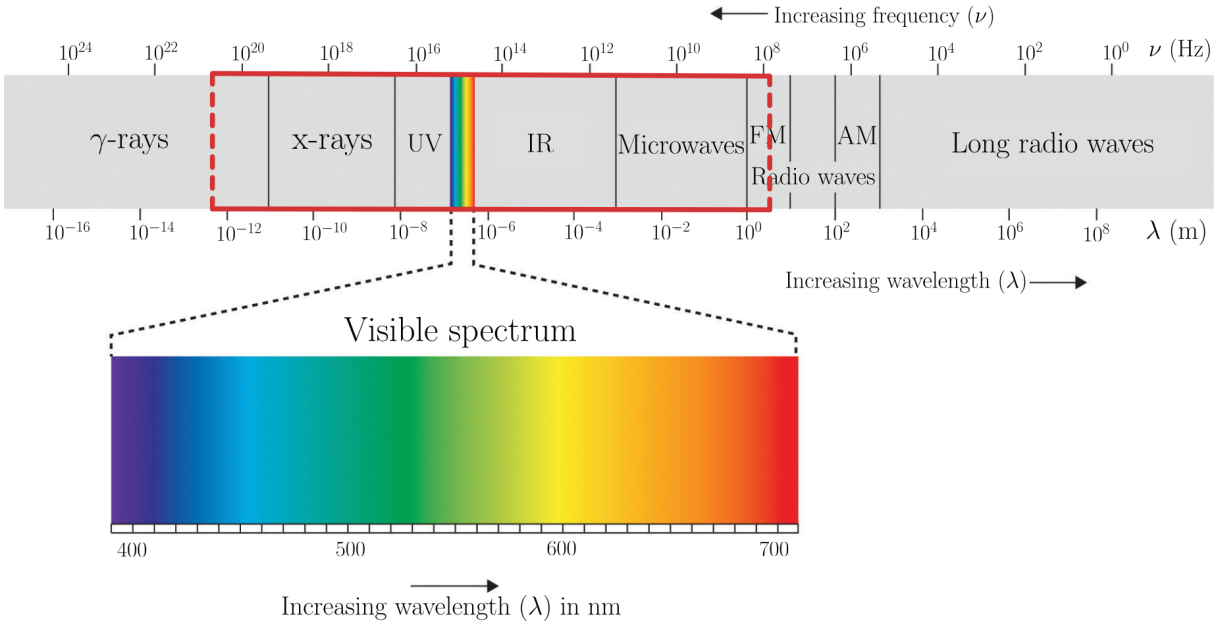

Figure 2: EM spectrum with synchrotron region highlighted in red. Credit: University of Minnesota (CC BY-NC-SA 4.0, modified).

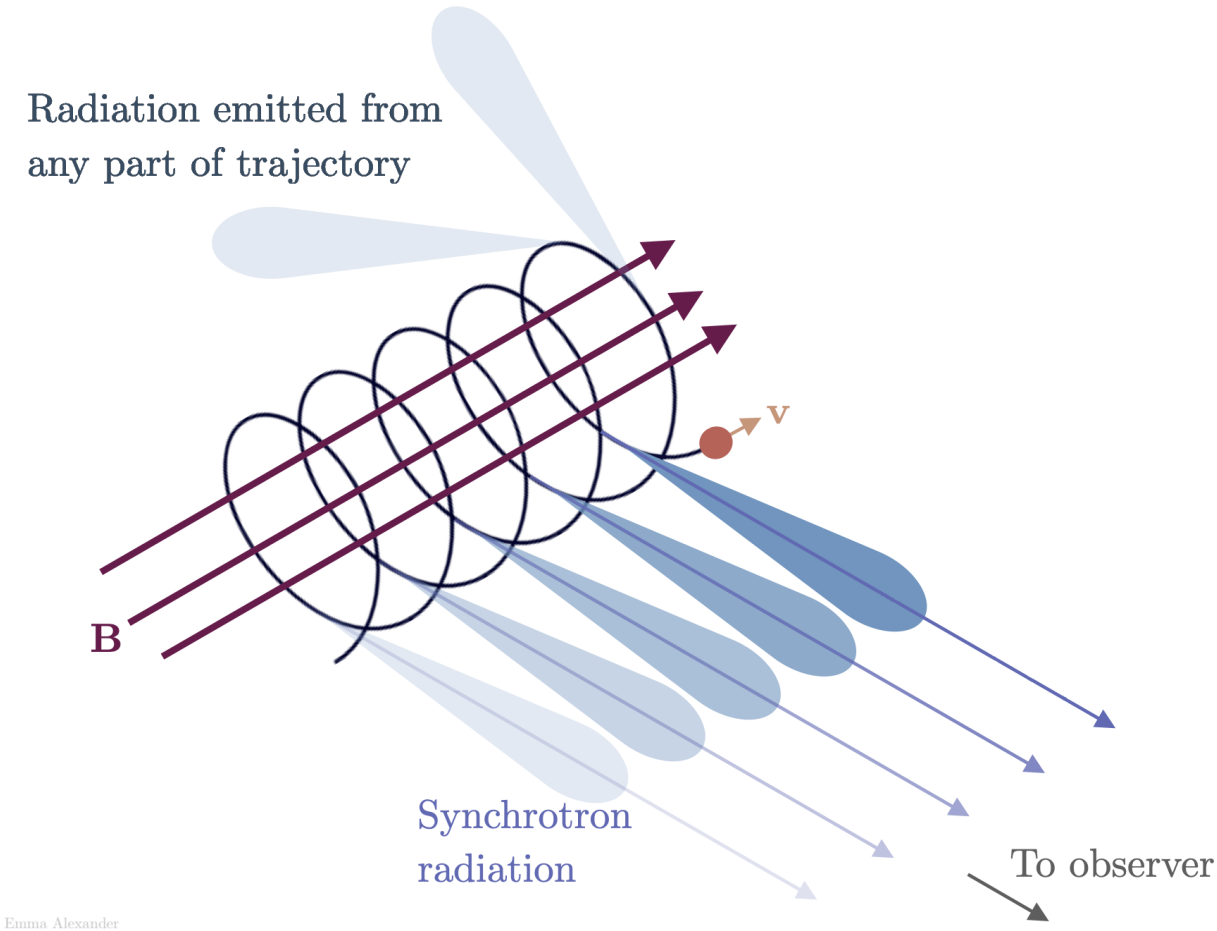

Figure 3: An electron gyrating through a magnetic field **B** at a velocity v which approaches the speed of light. Credit: Emma Alexander (CC BY 4.0, modified).

at $0.999c$. This time is defined as [11, Ch. 4]

$$\Delta t_{\text{observer}} = \gamma \Delta t_{\text{clock}}$$

and would be approximately 22 times greater than the time which is measured in the clock's rest frame. This is due to the effect of time dilation, a prediction of special relativity.

1.4 Relativistic Beaming

Relativistic beaming, or relativistic doppler effect, is a phenomenon that occurs when light is emitted from relativistic sources. In the case of GRBs, it affects what portion of the jet is visible to the observer. In short, an observer at rest compared to the epicenter of the explosion can only ever observe a cone of half angle $1/\gamma$ rad where γ is the Lorentz factor of the ejecta. The whole jet with half angle θ_j rad is not visible immediately [11, Ch. 4]. This is illustrated in Fig. 4.

This occurs as a consequence of the idea that the speed of light is constant in all reference frames, as posited by the theory of special relativity. The jet is moving with Lorentz factor $\gamma \gg 1$ [2] which means that from the observer frame, it will be measured slower by a factor γ than it is in its own rest frame. The light of the jet reaches the observer before the jet has had time to expand from the observers perspective. The slower the jet gets, the less pronounced this effect becomes because $1/\gamma$ approaches 1 as γ decreases [11, Ch. 4]. An illustration of the temporal evolution of this viewable cone is in Fig. 5

The way this expansion behaves depends on wether the jet is viewed on- or off-axis. Being on-axis means observing the jet coming toward you, while off-axis means viewing from the side. Granot, Panaitescu, Kumar, *et al.* [12] discuss the different light curves that occur depending on viewing axis. For an on-axis observer, they expect the light curve to be a steady power-law decline with a small break at t_{jet}, the point where the viewable cone of angle $1/\gamma$ becomes as large as the physical jet. After t_{jet} there is a second, steeper power-law function with no further breaks. For an off-axis observer, they expect a more pronounced break the farther off axis the observer is. After a certain observer angle is

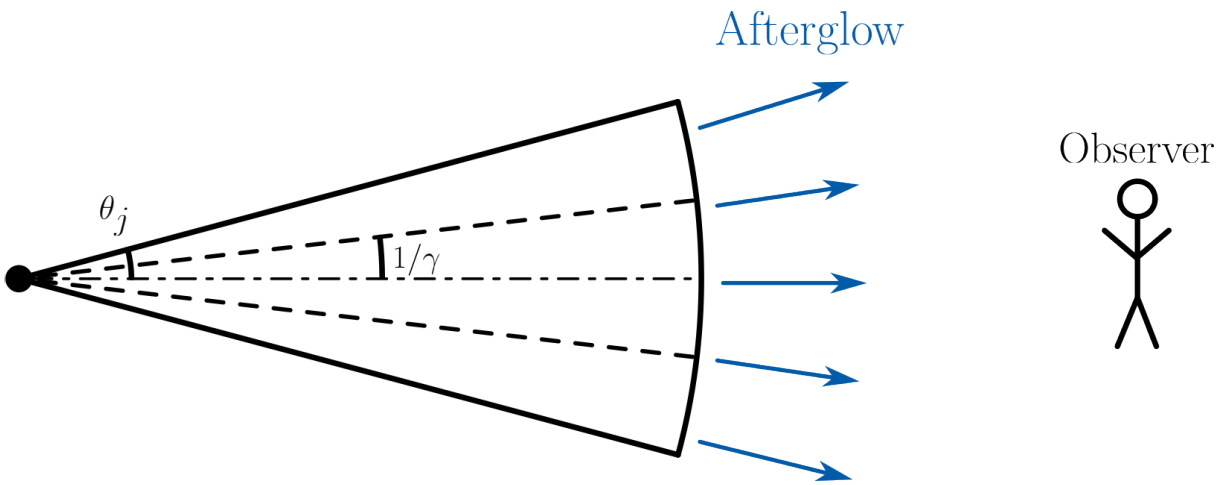

Figure 4: A relativistic jet beamed from a point source. Its exit angle is θ_j. Due to relativistic beaming the observer sees only a small part of the jet with an angle $1/\gamma$ where γ is the Lorentz factor of the jet.

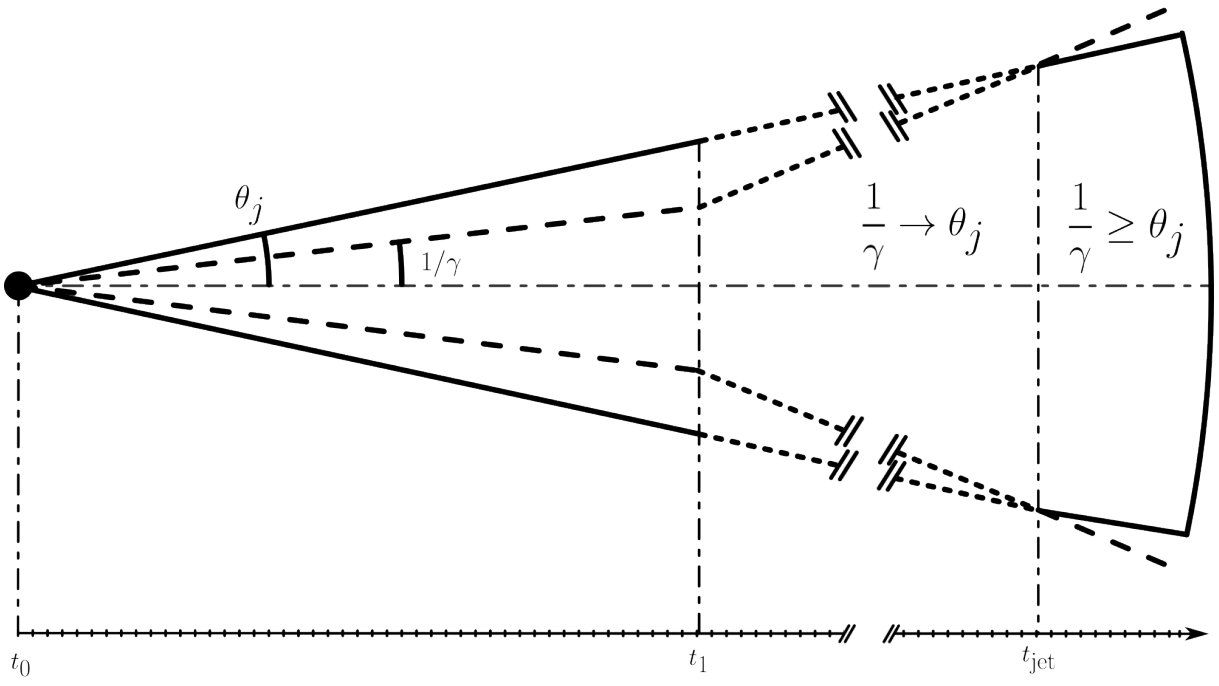

Figure 5: The temporal expansion of a GRB jet. Emission starts at time t_0. At some time t_1 only part of the jet can be observed, an angle of $1/\gamma$, due to relativistic beaming. As the jet decelerates γ gets smaller thus the viewable area increases. At a time t_{jet} the entire jet is visible. The viewable cone expands past this point and decreases flux over time.

reached, the the slope of the first power-law will become positive. This causes a peak in the light curve at t_{jet}

2 Calculations

This study is based on two articles: [1], [2]. The former discusses a spherical model of GRB afterglows and the latter a simple jet model. Both studies model afterglows with a combination of pure theory and observational fitting. The underlying equations are known in theory and numeric scaling factors that were fitted to data. Both studies [1] and [2] consider a power-law distribution of electron Lorentz factors γ_e with a logarithmic slope p moving through the ISM of density $n\,\mathrm{cm}^{-3}$. This distribution is in a magnetic field $B = \gamma_j c\sqrt{32\pi m_p \epsilon_b n}$ where ϵ_b is the fraction of jet energy imparted to the magnetic field and m_p is the proton mass. They move with the ejecta whose Lorentz factor is γ_j. The minimum Lorentz factor for this distribution is given as

$$\gamma_m = \epsilon_e \left(\frac{p-2}{p-1}\right) \frac{m_p}{m_e} \gamma_j \tag{1}$$

where m_e is the electron mass. Practically all emitting electrons reside above this factor [13]. For each emitting electron, the power and frequency of emission are given by

$$P(\gamma_e) = \frac{4}{3}\sigma_T c \gamma_j^2 \gamma_e^2 \frac{B^2}{8\pi}, \tag{2}$$

$$\nu(\gamma_e) = \gamma_j \gamma_e^2 \frac{q_e B}{2\pi m_e c}, \tag{3}$$

as shown in [1], [11, Ch. 6]. Here, σ_T is the Thomson scattering cross section and q_e is the electron charge.

When radiation is emitted the electron loses energy—it cools down. Electrons in the shock can only cool if their Lorentz factor is greater than the cooling, or critical, Lorentz factor γ_c, as stated by [1]. They give this factor as

$$\gamma_c = \frac{6\pi m_e c}{\sigma_T \gamma_j B^2 t}, \tag{4}$$

where t is observer time. Eventually, all electrons that have started to cool will cool to γ_c over the time t [1]. If $\gamma_c < \gamma_m$, then all electrons will cool to γ_c since they start above γ_c. This is called fast cooling. If $\gamma_c > \gamma_m$, not all electrons will meet the cooling threshold and only some will cool, this is slow cooling.

Two cases are considered in [1] for the energy evolution in the ejecta: a fully radiative and a fully adiabatic case. In this study, only the adiabatic case is considered. An adiabatic evolution is one where the total energy in the ejecta is constant. This energy is given in [1] as $E = 16\pi\gamma_j^2 R^3 n m_p c^2/17$ where m_p is the proton mass and R is the radius of the ejecta from the core as given in (5).

As shown in Fig. 1, the ejecta is moving into a surrounding ISM. As the shockwave moves, it collects matter from the ISM. While the sphere expands, its radius is given in [1] as

$$R(t) \cong \left(\frac{17Et}{4\pi m_p nc}\right)^{1/4} \tag{5}$$

for an isotropic expansion where E is the energy of the ejecta and t is the observer time. The Lorentz factor of the ejecta decreases with time and is given by

$$\gamma_j(t) \cong \left(\frac{17E}{1024\pi n m_p c^5 t^3}\right)^{1/8}$$

The number of electrons that are swept up in the shockwave are

$$N_e = \frac{4\pi}{3} R^3 n,$$

for a spherical expansion.

2.1 Spherical Light Curve

For the spherical expansion described by Sari, Piran, and Narayan [1], the flux at the observer in $\mathrm{erg} \cdot \mathrm{s}^{-1} \cdot \mathrm{Hz}^{-1} \cdot \mathrm{cm}^{-2}$ is given by

$$F_\nu = \begin{cases} (\nu/\nu_c)^{1/3} F_{\nu,\max}, & \nu_c > \nu, \\ (\nu/\nu_c)^{1/2} F_{\nu,\max}, & \nu_m > \nu > \nu_c, \\ (\nu_m/\nu_c)^{-1/2} (\nu/\nu_m)^{-p/2} F_{\nu,\max}, & \nu_c > \nu_m, \end{cases} \tag{6}$$

for the fast cooling case and as

$$F_\nu = \begin{cases} (\nu/\nu_m)^{1/3} F_{\nu,\max}, & \nu_m > \nu, \\ (\nu/\nu_m)^{-(p-1)/2} F_{\nu,\max}, & \nu_c > \nu > \nu_m, \\ (\nu_c/\nu_m)^{-(p-1)/2} (\nu/\nu_c)^{-p/2} F_{\nu,\max}, & \nu > \nu_c, \end{cases} \tag{7}$$

for the slow cooling case. In both equations, $F_{\nu,\max} \equiv N_e P_{\nu,\max}/(4\pi d_o^2)$ is the maximum observed flux at an observer distance of d_o cm. The frequencies ν_m and ν_c are the electron emission frequencies at γ_e and γ_c respectively. This would be calculated as $\nu(\gamma_e)$ and $\nu(\gamma_c)$ in (3). $P_{\nu,\max}$ is the max power emitted by a single electron. It is defined as

$$P_{\nu,\max} \approx \frac{P(\gamma_e)}{\nu(\gamma_e)} = \frac{m_e c^2 \sigma_T}{3 q_e} \gamma_j B.$$

The functions $P(\gamma_e)$ and $\nu(\gamma_e)$ are defined in (2) and (3) respectively. Note that $P_{\nu,\max}$ is independent of γ_e. This also makes $F_{\nu,\max}$ independent of γ_e. Thus, the above expressions in (6) and (7) are also independent of γ_e because ν is a free parameter. If $F_{\nu,\max}$ is evaluated for every frequency it returns the spectrum of emission at a constant time t. Evaluating for all t at one frequency returns the light curve which is of interest here.

2.2 Jet Light Curve

In the jet model found in [2], they focus on the critical and minimum frequencies ν_m and ν_c instead of the corresponding Lorentz factors. These are given as

$$\nu_m = \frac{q_e B}{m_e c}\gamma_e^2\gamma_j, \tag{8}$$

$$\nu_c = \frac{36\pi^2 q_e m_e c}{\gamma_j B^3 t^2}. \tag{9}$$

For the jet, the peak flux becomes independent of N_e and is given by [2] as

$$F_{\nu,\max} = \frac{2\sigma_T m_e c^2}{\pi q_e}\frac{R^3 n B\gamma_j}{d_o^2}. \tag{10}$$

Sari, Piran, and Halpern [2] state that for jets, $\nu_c \gg \nu_m$ for late times, that is, more than the first few hours. This is because ν_c is constant in time for an expanding jet. Then, the equation for flux at a given frequency is given as

$$F_\nu = \begin{cases} F_{\nu_m}(\nu/\nu_m)^{-(p-1)/2}, & \nu_m < \nu < \nu_c, \\ F_{\nu_c}(\nu_c/\nu_m)^{-(p-1)/2}, & \nu_m < \nu_c < \nu, \end{cases} \tag{11}$$

where p is the electron Lorentz factor distribution slope and ν can be calculated with (3). The main difference here is that [2] does not seem to consider fast and slow cooling, unlike [1].

3 Example Light Curves

To illustrate how GRB light curves can look, simulations were run using the jet model presented in [14]. The model was executed for the on-axis case with the parameters in Tab. 1 and for the off-axis case with the values in Tab. 2. All parameters were chosen arbitrarily to show the characteristic shape, so they do not necesarily reflect a specific real GRB. Despite this, all parameters in Tabs. 1 and 2 are possible to see in reality and thus provide a good example. Note that this model uses the redshift z instead of the observer

distance d_o, but these quantities are equivalent since redshift correlates to distance.

The resulting light curves are plotted in Fig. 6. Observing the dashed red lines, one can see the characteristic shapes as defined in Section 1.4. Observe that both curves have a break at $t \approx 11\,\mathrm{d}$, this is due to the fact that all parameters are identical except viewing angle θ_{obs}. Since $1/\gamma = \theta_{\mathrm{jet}}$ should occur at the same time no matter where one is looking from, at a constant distance, this is the expected result.

An approximation of the spherical model in [1] was made in Fig. 7. Here, the parameters were mostly the same as the typical values presented in [1]. Ultimately, the values used were arbitrary to show the characteristic shape.

Table 1: Input parameters for on-axis simulation. The cosmological redshift z was used here instead of the observer distance d_o.

Parameter	**Value**
z	0.065
θ_{obs}	$0.01\,\mathrm{rad}$
θ_{jet}	$0.1\,\mathrm{rad}$
E_0	$1 \times 10^{53}\,\mathrm{erg}$
n	$1 \times 10^{-5}\,\mathrm{cm}^{-3}$
p	2.5
ϵ_e	0.01
ϵ_b	0.01
γ_0	500
ν	$2 \times 10^{17}\,\mathrm{Hz}$

Table 2: Input parameters for off-axis simulation. The cosmological redshift z was used here instead of the observer distance d_o.

Parameter	**Value**
z	0.065
θ_{obs}	$0.2\,\mathrm{rad}$
θ_{jet}	$0.1\,\mathrm{rad}$
E_0	$1 \times 10^{53}\,\mathrm{erg}$
n	$1 \times 10^{-5}\,\mathrm{cm}^{-3}$
p	2.5
ϵ_e	0.01
ϵ_b	0.01
γ_0	500
ν	$2 \times 10^{17}\,\mathrm{Hz}$

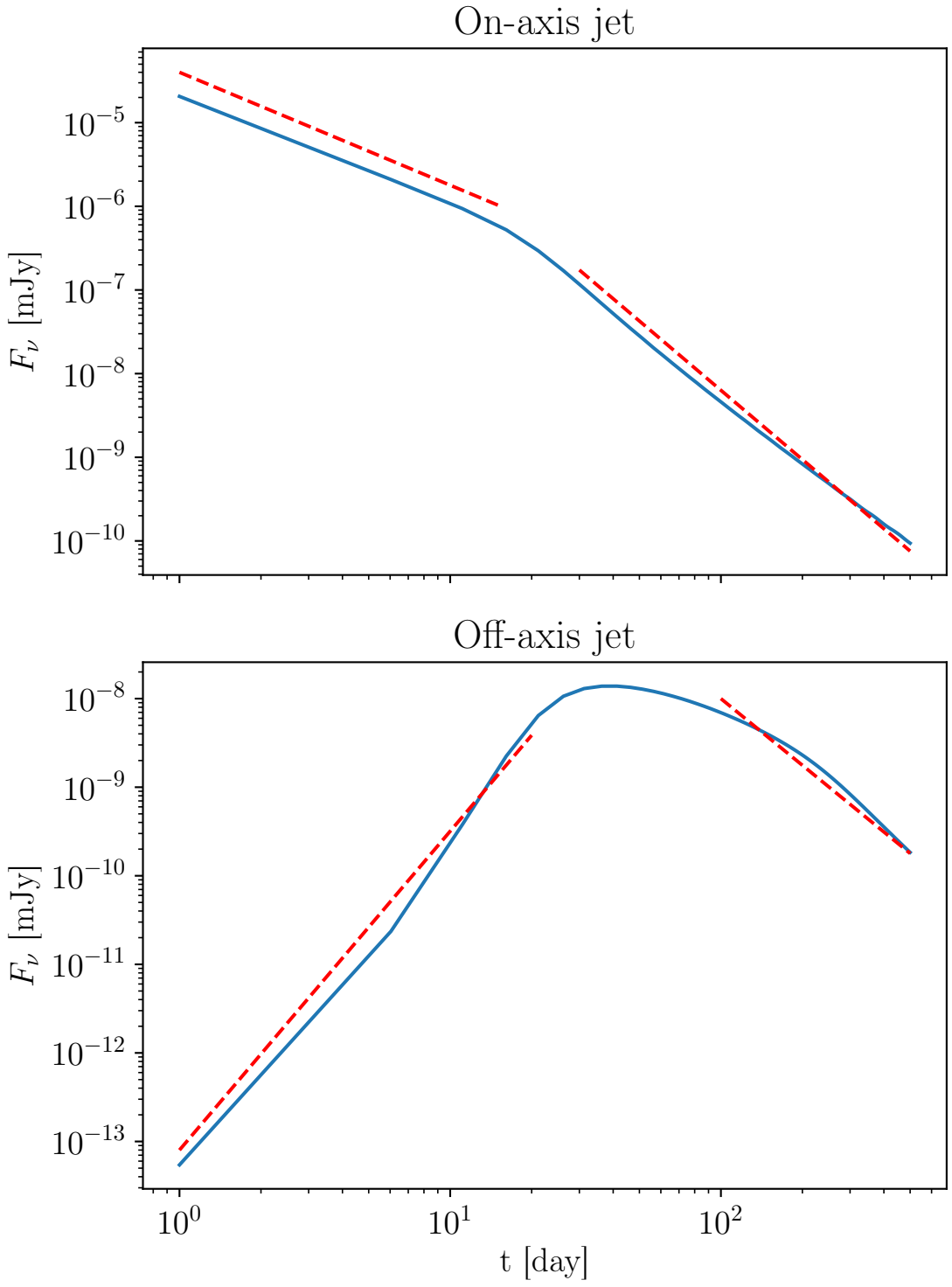

Figure 6: The light curves for on- and off-axis jet models. The dashed red lines indicate guesses at the approximate slop for their domain. This figure is for illustration purposes only, the data in it is not realistic.

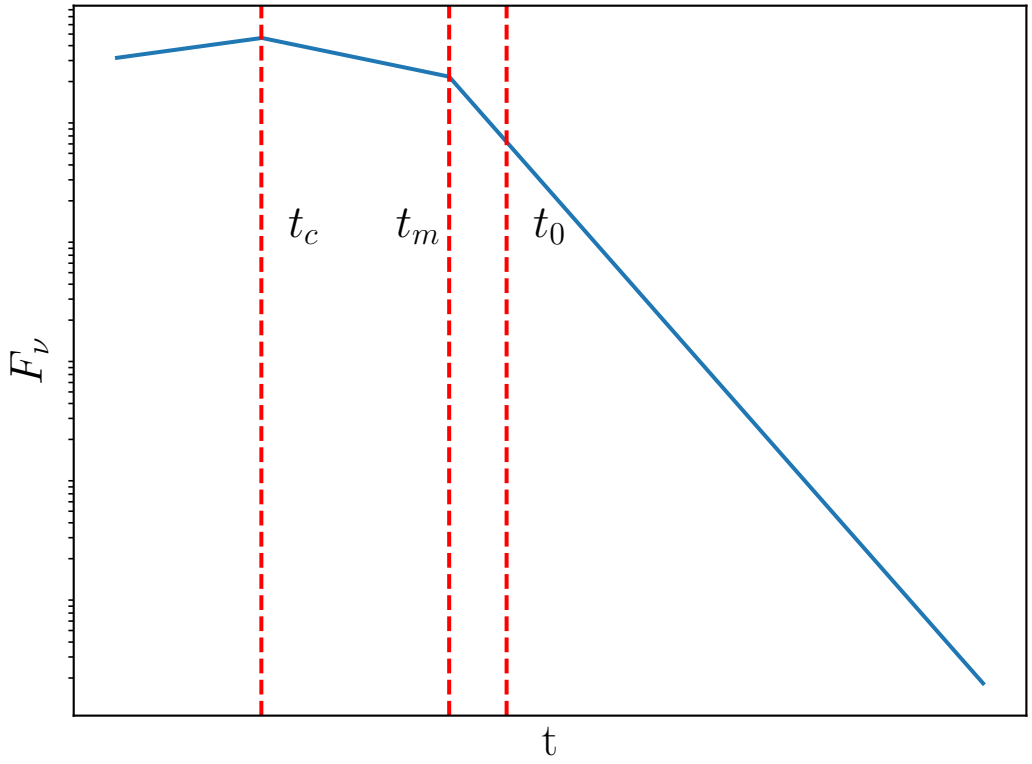

Figure 7: The shape of a light curve for a spherical model. This data has no direct correlation to reality but was chosen arbitrarily with parameters similar to those in [1]. The time t_0 is when the afterglow shifts from slow to fast cooling. The times t_c and t_m are when ν_c and ν_m respectively cross the observed frequency ν.

4 Discussion

Being able to model GRB afterglows gives us insight into the physics of the explosions that create them. Kilonovae and supernovae are a fundamental part of the evolution of the universe since they are essential in the creation of heavier elements than iron. Stars can usually only fuse elements lighter than iron. Iron fusion is endothermic and can therefore not sustain a star. Modern studies, such as [7], are starting to truly understand the heavy elements that come out of the events that cause GRBs.

Currently, the jet model of ejecta expansion is widely accepted [9]. The models in this paper assume an isotropic energy distribution in the ejecta. This is not the case in reality. Modern models, such as [15], show that there are different ”shells” that make up a jet. Each shell has a different energy level and radiates at a different spectrum. It is

also known that jets are not confined to their exit angle θ_j, but instead spread out past this ideal cone over time [16]. This is known as a structured jet and is an active field of reasearch. Further studies into jet structure could give more detailed insight on the physical processes involved in forming jets.

Furthermore, the progenitors of GRBs and the explosions they generate are other fields of intense study. The long GRB-supernova relation has been widely accepted [9]. The origin of short GRBs is less clear. Studies such as [7] are starting to solidify the idea that short GRBs are caused by kilonovae. However, how other possible progenitors relate to the type of GRB produced is still unclear [9].

With data from sattelites such as Fermi [17], [18] and Swift [19] as well as the recently launched James Webb Space Telescope (JWST) [20], there is a large amount of data to process. For example, the important discoveries by Levan, Gompertz, Salafia, *et al.* [7] were made using JWST data. The future of gamma-ray burst research is bright and there is a lot of potential for new discoveries.

References

[1] R. Sari, T. Piran, and R. Narayan, "Spectra and light curves of gamma-ray burst afterglows," *The Astrophysical Journal*, vol. 497, no. 1, pp. L17–L20, Mar. 1998. DOI: 10.1086/311269.

[2] R. Sari, T. Piran, and J. P. Halpern, "Jets in grbs," *The Astrophysical Journal*, vol. 519, no. 1, 1999. DOI: 10.1086/312109.

[3] B. Zhang, "The physics of gamma-ray bursts," in Cambridge University Press, 2019, ch. 1,2 and 8, ISBN: 978-1-107-02761-9. DOI: 10.1017/9781139226530.

[4] C. Kouveliotou, C. A. Meegan, G. J. Fishman, *et al.*, "Identification of two classes of gamma-ray bursts," *Astrophysical Journal Letters*, vol. 413, p. L101, Aug. 1993. DOI: 10.1086/186969.

[5] E. Costa, F. Frontera, J. Heise, *et al.*, "Discovery of an x-ray afterglow associated with the γ-ray burst of 28 february 1997," *Nature*, no. 387, pp. 783–785, 1997. DOI: 10.1038/42885.

[6] K. Z. Stanek, T. Matheson, P. M. Garnavich, *et al.*, "Spectroscopic discovery of the supernova 2003dh associated with grb 030329*," *The Astrophysical Journal*, vol. 591, no. 1, p. L17, Jun. 2003. DOI: 10.1086/376976. [Online]. Available: https://dx.doi.org/10.1086/376976.

[7] A. Levan, B. P. Gompertz, O. S. Salafia, *et al.*, "Jwst detection of heavy neutron capture elements in a compact object merger," 2023. DOI: 10.48550/arXiv.2307.02098.

[8] R. W. Klebesadel, I. B. Strong, and R. A. Olson, "Observations of gamma-ray bursts of cosmic origin," *The Astrophysical Journal*, vol. 182, p. L85, 1973. DOI: 10.1086/181225.

[9] N. Gehrels and P. Mészáros, "Gamma-ray bursts," *Science*, vol. 337, no. 6097, pp. 932–936, 2012. DOI: 10.1126/science.1216793.

[10] NIST. "What is synchrotron radiation?" (2010), [Online]. Available: https://www.nist.gov/pml/sensor-science/what-synchrotron-radiation (visited on 07/07/2023).

[11] G. B. Rybicki and A. P. Lightman, "Radiative processes in astrophysics," in Wiley-VCH, 1979, ch. 4 and 6, ISBN: 978-0-471-82759-7.

[12] J. Granot, A. Panaitescu, P. Kumar, and S. E. Woosley, "Off-Axis Afterglow Emission from Jetted Gamma-Ray Bursts," *The Astrophysical Journal*, vol. 570, no. 2, pp. L61–L64, May 2002. DOI: 10.1086/340991.

[13] R. Sari, R. Narayan, and T. Piran, "Cooling timescales and temporal structure of gamma-ray bursts," *The Astrophysical Journal*, vol. 473, no. 1, pp. 204–218, Dec. 1996. DOI: 10.1086/178136. [Online]. Available: https://doi.org/10.1086%2F178136.

[14] G. P. Lamb, D. A. Kann, J. J. Fernández, I. Mandel, A. J. Levan, and N. R. Tanvir, "GRB jet structure and the jet break," *Monthly Notices of the Royal Astronomical Society*, vol. 506, no. 3, pp. 4163–4174, Sep. 2021. DOI: 10.1093/mnras/stab2071.

[15] P. Kumar, "Gamma-ray burst energetics," *The Astrophysical Journal*, vol. 523, no. 2, p. L113, Aug. 1999. DOI: 10.1086/312265. [Online]. Available: https://dx.doi.org/10.1086/312265.

[16] O. S. Salafia and G. Ghirlanda, "The structure of gamma ray burst jets," *Galaxies*, vol. 10, no. 5, p. 93, 2022.

[17] C. Meegan, G. Lichti, P. Bhat, *et al.*, "The fermi gamma-ray burst monitor," *The Astrophysical Journal*, vol. 702, no. 1, p. 791, 2009.

[18] C. Meegan, G. Lichti, P. Bhat, *et al.*, "The fermi gamma-ray burst monitor," *The Astrophysical Journal*, vol. 702, no. 1, p. 791, 2009.

[19] N. Gehrels, G. Chincarini, P. e. Giommi, *et al.*, "The swift gamma-ray burst mission," *The Astrophysical Journal*, vol. 611, no. 2, p. 1005, 2004.

[20] J. P. Gardner, J. C. Mather, M. Clampin, *et al.*, "The James Webb Space Telescope," *Space Science Reviews*, vol. 123, no. 4, pp. 485–606, 2006. [Online]. Available: `https://doi.org/10.1007/s11214-006-8315-7`.